

High-Performance Lead-Free Piezoceramics with High Curie Temperatures

Myang Hwan Lee, Da Jeong Kim, Jin Su Park, Sang Wook Kim, Tae Kwon Song,*
Myong-Ho Kim, Won-Jeong Kim, Dalhyun Do, and Il-Kyoung Jeong

Piezoelectric materials convert electrical energy into mechanical energy and vice versa, and are applied to actuators and sensors.^[1–3] Lead-free piezoelectric materials have been studied to replace the commonly used lead zirconate titanate (PZT) because of environmental and health issues.^[2,4–7] Piezoelectric properties are usually inversely proportional to the phase transition Curie temperature (T_C),^[5–10] but PZT is an exception that has good piezoelectric properties with a high T_C . Here, we show that a bismuth ferrite (BF) and barium titanate (BT) solid solution system can achieve good piezoelectric properties with a high T_C when fabricated with low-temperature sintering followed by a water-quenching process, with no complicated grain alignment processes performed. By adding the super-tetragonal compound of bismuth gallium oxide, the piezoelectric properties were equal to that of PZT ceramics and exhibited good long-term reliabilities.

At the morphotropic phase boundary (MPB), where different crystal phases coexist, good piezoelectric properties are exhibited by piezoceramics because of the various ferroelectric switching paths that are available.^[11] For sodium potassium niobate (NKN)-based ceramics, polymorphic phase transition (PPT) has been used for the same purpose.^[7–9] Therefore, fabricating piezoceramics with chemical compositions around their MPB or PPT is an effective method for obtaining good piezoelectric properties.^[7–13] For the NKN-based system, the best performance ($d_{33} = 490 \text{ pC N}^{-1}$, $T_C = 227^\circ\text{C}$) was exhibited in $0.96(\text{Na}_{0.52}\text{K}_{0.48})\text{-(Nb}_{0.95}\text{Sb}_{0.05})\text{O}_3\text{-}0.04\text{Bi}_{0.5}(\text{Na}_{0.92}\text{K}_{0.18})_{0.5}\text{ZrO}_3$ (NKNSb) ceramic.^[9] A new tricritical-point-type MPB was reported for lead-free BT-based systems.^[14] For the $\text{Ba}(\text{Ti}_{0.8}\text{Zr}_{0.2})\text{O}_3\text{-(Ba}_{0.7}\text{Ca}_{0.3})\text{TiO}_3$

(BTZ-BCT) system, the piezoelectric charge sensor constant (d_{33}) is approximately 620 pC N^{-1} . However, T_C of this compound (93°C) is too low for real-world applications.^[14]

MPBs have been reported for pressurized lead titanate (PT)^[15] and thin films of BF, which was induced by substrate-imposed stresses.^[16] While enhanced piezoelectric properties were exhibited by these systems, applications requiring piezoelectric thin films are limited compared to bulk ceramics. In addition, applying an external pressure to a piezoelectric device is not practical. Therefore, bulk piezoelectric ceramics or thick films are widely used for actuators and sensors. However, there is an urgent need to develop high-performance lead-free piezoceramics with high T_C that can be easily synthesized. By using the reactive-templated grain growth (RTGG) method to fabricate lead-free NKN-based ceramics,^[10] a d_{33} higher than 300 pC N^{-1} and a T_C of 300°C was obtained. However, the RTGG method is too complicated and expensive for mass production. Thus, a piezoceramic has not yet been developed with the properties needed to replace PZT: $d_{33} > 300 \text{ pC N}^{-1}$, $T_C > 300^\circ\text{C}$ and a simple synthetic route.

The ferroelectric and (anti)ferromagnetic properties of BF ceramics and thin films have been studied in detail.^[17] The high T_C of BF allows the fabrication of high-temperature piezoceramics composed of a solid solution of BF and PT.^[18,19] In addition, a solid solution of BF and BT has been studied to develop high- T_C lead-free piezoceramics. However, the reported piezoelectric properties did not match those of PZT and there is not yet a consensus on the system's phase diagram.^[20–24] The volatile nature of bismuth and multiple valences of iron make sintering bulk BF-based ceramics difficult, and the high leakage currents in ions-modified BF ceramics are the main obstacle to obtaining good piezoelectric properties.^[25–27]

By doping a third material in BF-BT ceramics, we have tried to improve piezoelectric properties and to increase T_C . Bismuth-based oxides, such as bismuth scandate, have been studied as a part of solid solutions with PT to develop high-temperature piezoceramics.^[28–30] The T_C of some of these solid solution systems exceeded that of PZT. However, these bismuth-based ceramics are very difficult to make with conventional ceramic processing. Thus, high-pressure sintering has been used to fabricate bismuth-based ceramics.^[28,31] Super-tetragonal materials, such as bismuth zinc titanate $[\text{Bi}(\text{Zn}_{0.5}\text{Ti}_{0.5})\text{O}_3]$, BZT^[32] and bismuth gallium oxide (BiGaO_3 , BG),^[33] are strong candidates as the third material in the ternary system because they complement BT, which has low tetragonal distortion (c_T/a_T) and low T_C .

Figure 1a shows a comparison of the d_{33} values of the piezoceramics at 25°C with respect to their T_C . This figure is a modified reproduction of Figure 1b from a letter by Saito et al.^[10] The down-triangles represent the conventional lead-free

Dr. M. H. Lee, D. J. Kim, J. S. Park,
Prof. T. K. Song, Prof. M.-H. Kim
School of Materials Science and Engineering
Changwon National University
Changwon, Gyeongnam 641-773, South Korea
E-mail: tksong@changwon.ac.kr

S. W. Kim, Prof. W.-J. Kim
Department of Physics
Changwon National University
Changwon, Gyeongnam 641-773, South Korea

Prof. D. Do
Department of Advanced Materials Engineering
Keimyung University
Daegu 704-701, South Korea

Prof. I.-K. Jeong
Department of Physics Education
Pusan National University
Busan 609-735, South Korea

DOI: 10.1002/adma.201502424



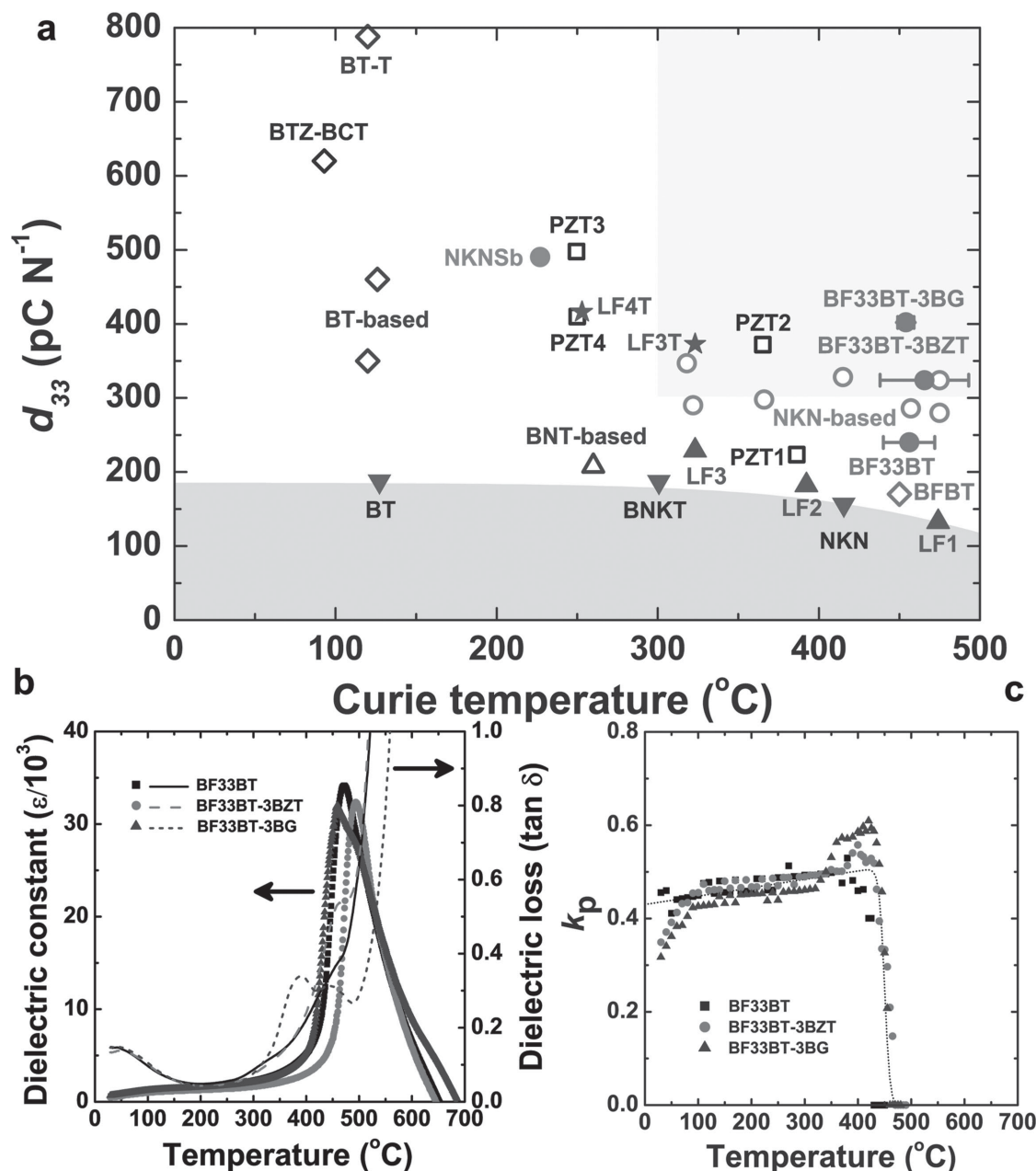


Figure 1. Piezoelectric properties (d_{33}) and Curie temperatures (T_C) of various piezoceramics. a) The d_{33} at 25 °C versus T_C . Filled circles = BF33BT, BF33BT-3BZT, and BF33BT-3BG ceramics. Filled down-triangles = BT, BNKT, and NKN piezoceramics.^[10] Filled up-triangles and stars = NKN-based ceramics fabricated without (LF1, LF2, and LF3) and with templates (LF3T and LF4T), respectively.^[10] Empty squares = PZT ceramics (PZT1, PZT2, PZT3, and PZT4).^[10] Empty diamond = BTZ-BCT ceramic.^[14] Empty diamonds = Oriented BT ceramic (BT-T) made by TGG method and BT-based ceramics.^[34–36] Filled circle = NKN ceramic with Sb (NKNSb).^[9] Empty circles = NKN-based ceramics without Sb.^[38–45] Empty diamond = BFBT ceramic.^[46] b) The ϵ (symbols) and $\tan\delta$ (lines) of BF33BT and ternary ceramics versus temperature on heating runs. c) The k_p of BF33BT and ternary ceramics versus temperature. Dotted line = eye-guide.

family of BT, NKN, and $\text{Bi}_{0.5}(\text{Na,K})_{0.5}\text{TiO}_3$ (BNKT) ceramics. The empty squares correspond to the commercially available PZT family. The up-triangles and stars represent NKN-based ceramics that were fabricated without and with the RTGG method, respectively.^[10] The recently developed BTZ-BCT system is represented by the empty black diamond.^[14] BT-based ceramics were denoted as empty diamonds.^[34,35] With template grain growth (TGG) method $d_{33} = 788$ pC N⁻¹ was obtained in

grain-oriented BT ceramic, but these BT-based systems also have problem of too low T_C .^[36] The best result in BNT-based system was denoted as an empty triangle.^[37] A recent progress in NKN-based system of NKNSb was denoted as a filled circle.^[9] The results of NKN-based ceramics without toxic antimony (Sb) were denoted as empty circles.^[38–45] But these NKN-based ceramics are sensitive to temperature because PPT has been used around room temperature.^[45]

On the other hand, the best performance reported for 0.65BF-0.35BT ceramic was 170 pC N^{-1} with a T_C of 450°C (BFBT, empty diamond).^[46] The filled circles are the data obtained in the present study. The d_{33} value of our 0.67BF-0.33BT ceramic (BF33BT FC) fabricated with a conventional furnace-cooling process was less than 200 pC N^{-1} .^[46] However, by using a water-quenching process (BF33BT in Figure 1a), the d_{33} and T_C increase to 240 pC N^{-1} and 456°C , respectively. In addition, we found that the piezoelectric properties are further improved by adding 3 mol% of either of the super-tetragonal BZT (BF33BT-3BZT, $d_{33} = 324 \text{ pC N}^{-1}$, $T_C = 466^\circ\text{C}$) or BG (BF33BT-3BG, $d_{33} = 402 \text{ pC N}^{-1}$, $T_C = 454^\circ\text{C}$). The d_{33} values of these ternary ceramics are as high as those of PZT ceramics, while their T_C values are higher than those of PZT ceramics.

The T_C values of the BF33BT and ternary ceramics were determined from the peak temperature of their temperature-dependent dielectric constant, $\epsilon(T)$ curves. Figure 1b shows

$\epsilon(T)$ and the dielectric loss, $\tan\delta(T)$, as functions of temperature. The T_C values plotted in Figure 1a are the averaged peak temperatures of the heating and cooling runs. The T_C values were also confirmed with high-temperature X-ray diffraction (XRD) measurements (Figures S1 and S2, Supporting Information).

The d_{33} value of the BF33BT ceramic increases from 240 pC N^{-1} at 25°C to 360 pC N^{-1} at 150°C .^[47] This improvement in d_{33} also occurred with the ternary ceramics as the temperature increased from 25 to 150°C : from 324 to 563 pC N^{-1} for the BF33BT-3BZT and from 402 to 645 pC N^{-1} for the BF33BT-3BG (Figure S3, Table S1, Supporting Information). We measured the temperature-dependent electromechanical coupling factor, $k_p(T)$, which increases with increasing temperature and then rapidly decreases at T_C .

As shown in Figure 2a, the samples have good polarization-electric field (P - E) ferroelectric hysteresis loops. The remnant polarizations (P_r) range from 0.19 to 0.24 C m^{-2} and the coercive

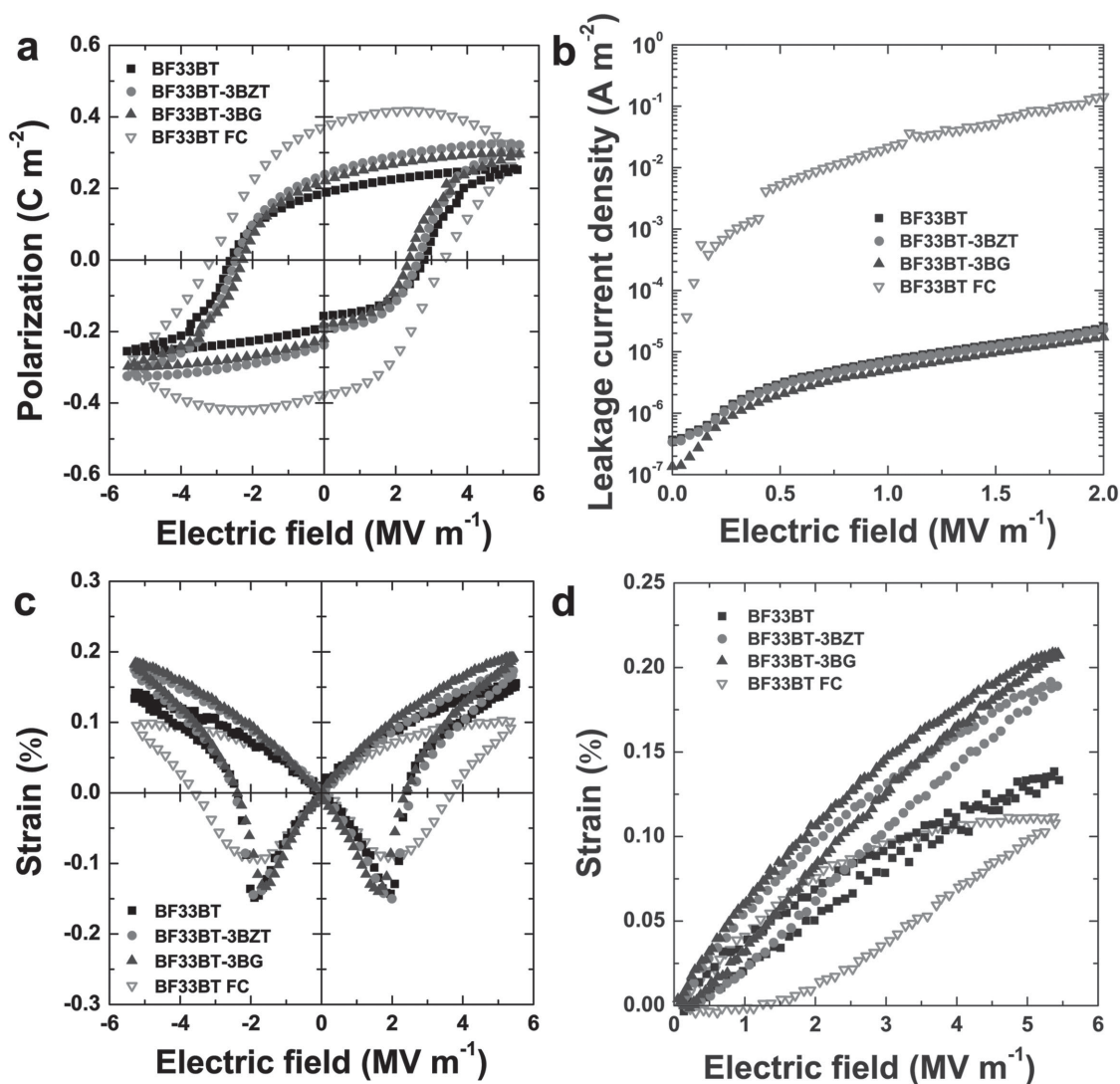


Figure 2. Ferroelectric and piezoelectric properties of the BF33BT ceramics. a) Ferroelectric P - E hysteresis loops of furnace-cooled (BF33BT FC), water-quenched BF33BT, BF33BT-3BZT, and BF33BT-3BG ceramics. b) Leakage current density behaviors of BF33BT FC, and BF33BT, BF33BT-3BZT, and BF33BT-3BG ceramics. c) Piezoelectric actuator responses of the bipolar S - E hysteresis loops. d) Piezoelectric actuator responses of unipolar S - E hysteresis loops.

fields (E_c) range from 2.4 to 2.8 MV m⁻¹. Water-quenched BF33BT and ternary ceramics exhibit leakage currents approximately three orders of magnitude smaller than that of the furnace-cooled ceramic (Figure 2b). The leakage current mechanism was analyzed on space charge limited conduction (Figure S4, Supporting Information). These reduced leakage currents made the poling process easier and may be a factor in the improved piezoelectric properties. In addition, the bipolar strain-electric field (S - E) responses are consistent with P - E loops (Figure 2c). The piezoelectric actuator constants (d_{33}^*) were measured from the unipolar S - E response results shown in Figure 2d.

The MPB or PPT composition of the (1- x)BF- x BT (BF-BT) water-quenched binary ceramic system was determined by measuring the piezoelectric properties of various samples with x ranging from 0.20 to 0.50. The highest d_{33} (240 pC N⁻¹) is exhibited by the sample with $x = 0.33$ (Figure 3a), and rhombohedral and tetragonal phases coexistence was confirmed with XRD measurements (Figure S5, Supporting Information). In XRD refinements by Rietveld analyses, peaks were fitted well with mixed phases as shown in Figure S6, Supporting Information. As shown in Figure 3b, the T_C is linearly dependent on x . When $x = 0.20$, the crystal structure is rhombohedral and the sample exhibits a hard P - E loop (Figure 3c). The highest d_{33}^* (375 pm V⁻¹) is obtained when $x = 0.40$, which exhibits a soft P - E loop and has a tetragonal crystal structure. This composition has the highest polarizations (Figure 3c) and S - E response (Figure 3d).

Based on the T_C measured from Figure 3b and the high-temperature XRD results, the phase diagram of the BF-BT system in BF-rich region was estimated (Figure 4a). From our $\epsilon(T)$ (red circles), high-temperature XRD data (orange diamonds) and data of Kumar et al.,^[20] Leontsev and Eitel,^[21] and Zhang et al.,^[23] the T_C values were obtained. The MPB or PPT is thought to be at $x = 0.33$ because the highest d_{33} value (brown star) was obtained and the phases coexist. It is apparent that water-quenching is likely to improve the piezoelectric properties because bismuth is less volatile.^[48,49] By the thermodynamic stability study of BF, it was found that BF has unstable temperature region between 447 and 767 °C, where Bi-rich and Fe-rich phases are more thermodynamically stable than BF.^[50] As a result, water-quenched BF ceramics have better ferroelectric properties.^[51] The low sintering temperature of 980–1010 °C is another advantage of the BF-BT system because it is necessary to use low temperature when cofiring multilayer electroceramics with internal metal electrodes are fabricated.

The structural properties of the BF33BT and ternary ceramics were analyzed and are summarized in Figure 4b,c. Compared to those of the furnace-cooled ceramic, all lattice constants (a_R , a_T , and c_T) of the rhombohedral and tetragonal phases in water-quenched ceramics have increased. It has been reported that the ferroelectric properties are strongly related to the tetragonal distortion (c_T/a_T) in tetragonal ferroelectric materials.^[17]

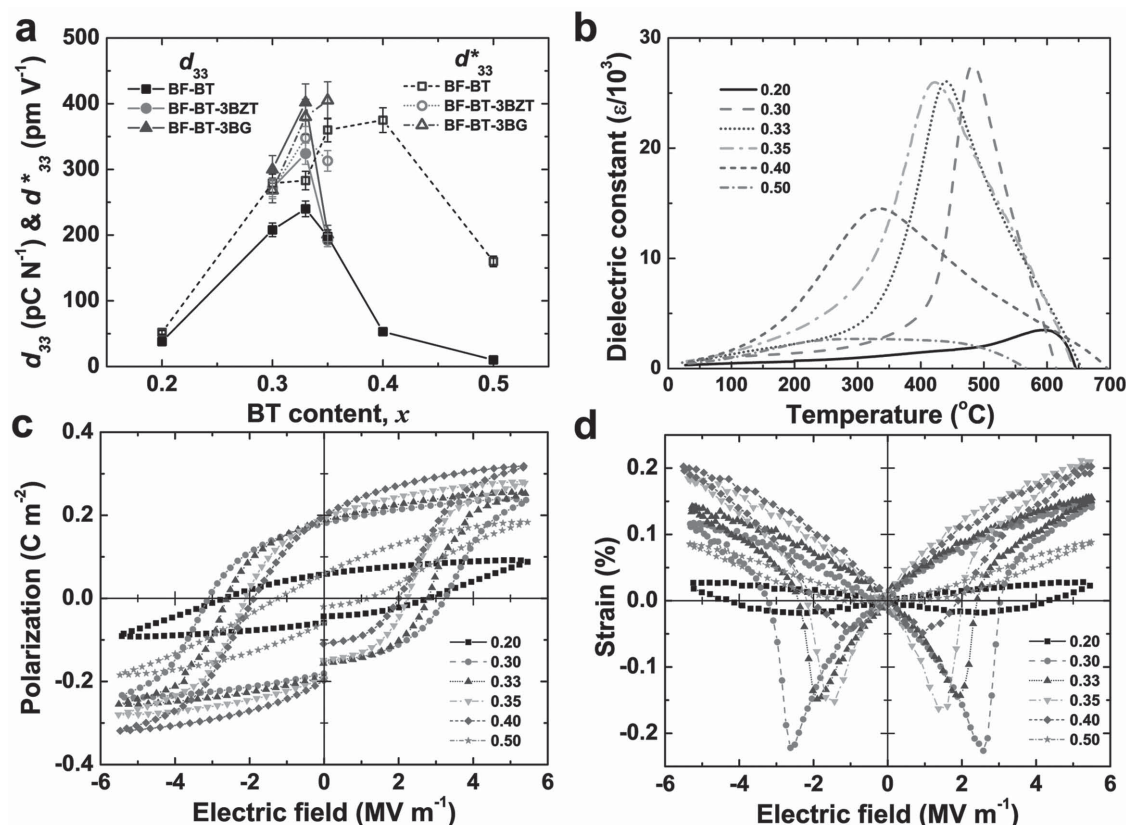


Figure 3. BT content (x)-dependent piezoelectric and ferroelectric properties of the BF-BT ceramics. a) The d_{33} (filled symbols) and d_{33}^* (empty symbols) values of the BF-BT, BF-BT-3BZT, and BF-BT-3BG ceramics as functions of x . b) Temperature-dependent dielectric constants of the BF-BT ceramics. c) Ferroelectric P - E hysteresis loops of the BF-BT ceramics. d) Bipolar S - E responses of the BF-BT ceramics.

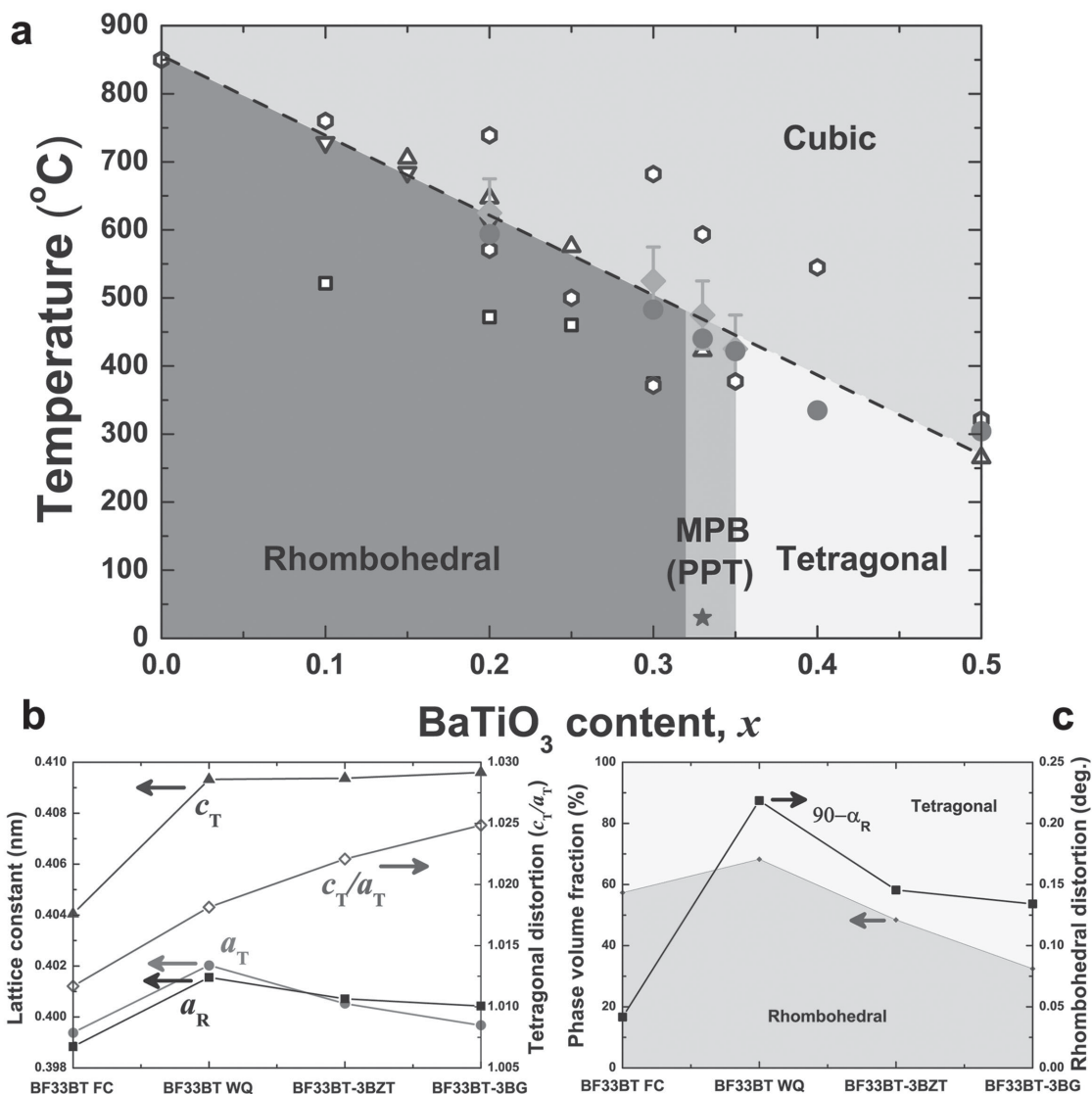


Figure 4. Phase diagram of the BF-BT system and structural properties of the BF33BT ceramics. a) Suggested phase diagram of the BF33BT system based on our experimental data (filled circles and filled diamonds) and that of Kumar et al.^[20] (empty black squares), Leontsev and Eitel^[21] (empty triangles), and Zhang et al.^[23] (empty hexagons). The star denotes the best d_{33} measured at room temperature. b) Lattice constants (a_R , a_T , and c_T) and tetragonal distortions (c_T/a_T). c) Rhombohedral distortions ($90^\circ - \alpha_R$) and phase volume fractions of furnace-cooled BF33BT FC, water-quenched BF33BT, BF33BT-3BZT, and BF33BT-3BG ceramics.

The water-quenching process has increased c_T/a_T from 1.012 to 1.018.

By adding the super-tetragonal compounds of BZT and BG to the BF33BT, the level of c_T/a_T increased further (Figure 4b and Figure S7, Supporting Information). The BF33BT-3BG sample exhibits the highest c_T/a_T of 1.025. The rhombohedral distortion, $90^\circ - \alpha_R$ also increases from 0.042° to 0.219° . These increased structural distortions are attributed to the improvement of ferroelectric and piezoelectric properties.

The long-term reliability is also an important factor for real-world applications. The P - E loops after 10^0 , 10^4 , and 10^6 fatigue cycles are plotted in Figure S8a, Supporting Information. After applying bipolar cycles of alternating electric fields, the P_r of the BF33BT ceramics remains at magnitudes of 0.25 C m^{-2} (Figure S8b, Supporting Information). The variations of d_{33}

values of BF33BT, BF33BT-3BZT, and BF33BT-3BG ceramics with and without poling process are plotted in Figure S8c, Supporting Information. These results show the BF33BT ceramics are resistant to fatigue cycles.

Experimental Section

Materials: The $0.67\text{Bi}_{1.05}\text{FeO}_3\text{-}0.33\text{BaTiO}_3$ (BF33BT), $(1-x)[0.67\text{Bi}_{1.05}\text{FeO}_3\text{-}0.33\text{BaTiO}_3]\text{-}x\text{Bi}_{1.05}(\text{Zn}_{0.5}\text{Ti}_{0.5})\text{O}_3$ ($x = 0.03$, BF33BT-3BZT), and $0.67\text{Bi}_{1.05}\text{FeO}_3\text{-}0.33\text{BaTiO}_3\text{-}x\text{Bi}_{1.05}(\text{Ga}_{0.5}\text{Ti}_{0.5})\text{O}_3$ ($x = 0.03$, BF33BT-3BG) ceramics were prepared from analytical grade metal oxide powders of Bi_2O_3 , Fe_2O_3 , BaCO_3 , TiO_2 , ZnO , and Ga_2O_3 (>99.9%, Sigma-Aldrich) with a transitional solid-state reaction method. We added 5 mol% of excess Bi to compensate for its volatility during the heat treatments. The powders were wet-mixed thoroughly in alcohol with a zirconia ball mill for 12 h. The mixtures were dried at 100°C and calcined at 700°C for 2 h. Polyvinyl alcohol (5 wt%)

was added to the calcined powders as a binding agent. The powders were pressed into disks with a diameter of 10 mm. The formed pellets were sintered for 3 h in air at 980–1010 °C depending on the composition (BF33BT = 980 °C, BF33BT-3BZT = 990 °C, and BF33BT-3BG = 1010 °C) and was followed by a water-quenching process.

Characterization: The phase composition of the sintered samples was identified with X-ray diffraction (XRD, D8 Discover, Bruker). The phase transition temperatures of the samples were examined with in situ high-temperature (25–700 °C) XRD. The crystal structures were analyzed with a Rietveld refinement program, Fullprof. From the Rietveld analysis of the mixed phases around the MPB or PPT, the peaks of the rhombohedral and tetragonal phases were deconvoluted and the structural properties were analyzed. For electrical measurements, the surfaces of the sintered ceramics were coated via ion sputtering with Pt and then coated again with silver paste. The ferroelectric hysteresis loops were measured at 10 Hz (Precision LC, Radiant). For the piezoelectric measurements, the samples were poled by applying a DC electric field of 6.6 MV m⁻¹ for 30 min in a silicone oil bath. The poling processes were the most effective at approximately 200 °C (the minimum tan $\delta(T)$ values as shown in Figure 1b). The d_{33} was measured with a d_{33} -meter (ZJ-6B, HC Materials). The leakage current was measured with a high-voltage source (248, Keithley) and an electrometer (6514, Keithley). The d_{33} was measured with a linear variable differential transformer (Millimar 1240, Mahr) at 50 mHz. The k_p was measured with a resonance method by using an impedance analyzer (HP4194A, Agilent). Temperature-dependent dielectric constants, $\epsilon(T)$ and losses, tan $\delta(T)$ were measured with computerized furnace system and an impedance analyzer (HP4194A, Agilent) with heating/cooling rates of 1 °C min⁻¹. Fatigue cycles of 5 MV m⁻¹ and 30 Hz were applied to study long-term reliabilities.

Supporting Information

Supporting Information is available from the Wiley Online Library or from the author.

Acknowledgements

This work was supported by a National Research Foundation of Korea (NRF) grant funded by the Korean government (Ministry of Science, ICT and Future Planning, MSIP No. 2012-0009457); the Priority Research Centres Program through the NRF funded by the Ministry of Education (MOE, 2013R1A1A4A01010612 and 2012-045424); and the Materials and Components Technology Development Program (10047914) of the Ministry of Trade, Industry and Energy (MOTIE), South Korea.

Received: May 20, 2015

Revised: August 24, 2015

Published online: October 7, 2015

- [1] B. Jaffe, W. R. Cook, H. Jaffe, *Piezoelectric Ceramics*, Academic Press, London, UK 1971.
- [2] S. Priya, S. Nahm, *Lead-Free Piezoelectrics*, Springer-Verlag, New York 2012.
- [3] C. K. Jeong, J. Lee, S. Han, J. Ryu, G.-T. Hwang, D. Y. Park, J. H. Park, S. S. Lee, M. Byun, S. H. Ko, K. J. Lee, *Adv. Mater.* **2015**, 27, 2866.
- [4] J. Rödel, W. Jo, K. T. P. Seifert, E.-M. Anton, T. Granzow, D. Damjanovic, *J. Am. Ceram. Soc.* **2009**, 92, 1153.
- [5] J. Rödel, K. G. Webber, R. Dittmer, W. Jo, M. Kimura, *J. Eur. Ceram. Soc.* **2015**, 35, 1659.
- [6] T. R. Shrout, S. J. Zhang, *J. Electroceram.* **2007**, 19, 111.
- [7] J. Wu, D. Xiao, J. Zhu, *Chem. Rev.* **2015**, 115, 2559.
- [8] X. Wang, J. Wu, D. Xiao, X. Cheng, T. Zheng, X. Lou, B. Zhang, J. Zhu, *ACS Appl. Mater. Interfaces* **2014**, 6, 6177.
- [9] X. Wang, J. Wu, D. Xiao, J. Zhu, X. Cheng, T. Zheng, B. Zhang, X. Lou, X. Wang, *J. Am. Chem. Soc.* **2014**, 136, 2905.
- [10] Y. Saito, H. Takao, T. Tani, T. Nonoyama, K. Takatori, T. Homma, T. Nagaya, M. Nakamura, *Nature* **2004**, 432, 84.
- [11] R. Guo, L. E. Cross, S.-E. Park, B. Noheda, D. E. Cox, G. Shirane, *Phys. Rev. Lett.* **2000**, 84, 5423.
- [12] P. Mandal, A. Manjón-Sanz, A. J. Corkett, T. P. Comyn, K. Dawson, T. Stevenson, J. Bennett, L. F. Henrichs, A. J. Bell, E. Nishibori, M. Takata, M. Zanella, M. R. Dolgos, U. Adem, X. Wan, M. J. Pitcher, S. Romani, T. T. Tran, P. S. Halasyamani, J. B. Claridge, M. J. Rosseinsky, *Adv. Mater.* **2015**, 27, 2883.
- [13] D. S. Keeble, E. R. Barney, D. A. Keen, M. G. Tucker, J. Kreisel, P. A. Thomas, *Adv. Funct. Mater.* **2013**, 23, 185.
- [14] W. Liu, X. Ren, *Phys. Rev. Lett.* **2009**, 103, 257602.
- [15] M. Ahart, M. Somayazulu, R. E. Cohen, P. Ganesh, P. Dera, H.-K. Mao, R. J. Hemley, Y. Ren, P. Liermann, Z. Wu, *Nature* **2008**, 451, 545.
- [16] R. J. Zeches, M. D. Rossell, J. X. Zhang, A. J. Hatt, Q. He, C.-H. Yang, A. Kumar, C. H. Wang, A. Melville, C. Adamo, G. Sheng, Y.-H. Chu, J. F. Ihlefeld, R. Erni, C. Ederer, V. Gopalan, L. Q. Chen, D. G. Schlom, N. A. Spaldin, L. W. Martin, R. Ramesh, *Science* **2009**, 326, 977.
- [17] G. Catalan, J. F. Scott, *Adv. Mater.* **2009**, 21, 2463.
- [18] T. P. Comyn, S. P. McBride, A. J. Bell, *Mater. Lett.* **2004**, 58, 3844.
- [19] L. Fan, J. Chen, S. Li, H. Kang, L. Liu, L. Fang, X. Xing, *Appl. Phys. Lett.* **2013**, 102, 022905.
- [20] M. M. Kumar, A. Srinivas, S. V. Suryanarayana, *J. Appl. Phys.* **2000**, 87, 855.
- [21] S. O. Leontsev, R. E. Eitel, *J. Am. Ceram. Soc.* **2009**, 92, 2957.
- [22] A. Singh, C. Moriyoshi, Y. Kuroiwa, D. Pandey, *Phys. Rev. B* **2013**, 88, 024113.
- [23] H. Zhang, W. Jo, W. Ke, K. G. Webber, *Ceram. Int.* **2014**, 40, 4759.
- [24] S. O. Leontsev, R. E. Eitel, *Sci. Technol. Adv. Mater.* **2010**, 11, 044302.
- [25] M. M. Kumar, V. R. Palkar, K. Srinivas, S. V. Suryanarayana, *Appl. Phys. Lett.* **2000**, 76, 2764.
- [26] R. Palai, R. S. Katiyar, H. Schmid, P. Tissot, S. J. Clark, J. Robertson, S. A. T. Redfern, G. Catalan, J. F. Scott, *Phys. Rev. B* **2008**, 77, 014110.
- [27] T. Rojac, M. Kosec, B. Budic, N. Setter, D. Damjanovic, *J. Appl. Phys.* **2010**, 108, 074107.
- [28] R. E. Eitel, C. A. Randall, T. R. Shrout, P. W. Rehrig, W. Hackenberger, S.-E. Park, *Jpn. J. Appl. Phys.* **2001**, 40, 5999.
- [29] M. R. Suchomel, P. K. Davies, *J. Appl. Phys.* **2004**, 96, 4405.
- [30] K. V. Lalitha, A. N. Fitch, R. Ranjan, *Phys. Rev. B* **2013**, 87, 064106.
- [31] Q. Zhou, C. Zhou, H. Yang, G. Chen, W. Li, H. Wang, *J. Am. Ceram. Soc.* **2012**, 95, 3889.
- [32] S. Yasui, K. Yazawa, M. Matsushima, T. Yamada, H. Morioka, H. Uchida, T. Iijima, L. You, J. Wang, T. Yamamoto, Y. Ikuhara, H. Funakubo, *Appl. Phys. Lett.* **2013**, 103, 042904.
- [33] A. A. Belik, D. A. Rusakov, T. Furubayashi, E. Takayama-Muromachi, *Chem. Mater.* **2012**, 24, 3056.
- [34] T. Karaki, K. Yan, M. Adachi, *Jpn. J. Appl. Phys.* **2007**, 46, 7035.
- [35] H. Takahashi, Y. Numamoto, J. Tani, K. Matsuta, J. Qiu, S. Tsurekawa, *Jpn. J. Appl. Phys.* **2006**, 45, L30.
- [36] S. Wada, K. Takeda, T. Muraishi, H. Kakemoto, T. Tsurumi, T. Kimura, *Ferroelectrics* **2008**, 373, 11.
- [37] D. Lin, K. W. Kwok, H. L. W. Chan, *Solid State Ionics* **2008**, 178, 1930.
- [38] K. Wang, J.-F. Li, *Adv. Funct. Mater.* **2010**, 20, 1924.
- [39] K. Wang, J.-F. Li, N. Liu, *Appl. Phys. Lett.* **2008**, 93, 092904.
- [40] X. Wang, J. Wu, Z. Lv, H. Tao, X. Cheng, T. Zheng, B. Zhang, D. Xiao, J. Zhu, *J. Mater. Sci. Mater. Electron.* **2014**, 25, 3219.
- [41] X. Cheng, J. Wu, X. Wang, B. Zhang, J. Zhu, D. Xiao, X. Wang, X. Lou, *Dalton Trans.* **2014**, 43, 3434.
- [42] Y. F. Chang, Z. Yang, D. Ma, Z. Liu, Z. Wang, *J. Appl. Phys.* **2008**, 104, 024109.
- [43] R. Z. Zuo, C. Ye, *Appl. Phys. Lett.* **2007**, 91, 062916.

- [44] W. Wang, X. Yuan, C. Ma, F. Tang, F. Wang, Y. Cao, *Ceram. Int.* **2015**, *41*, 8377.
- [45] K. Wang, F.-Z. Yao, W. Jo, D. Gobeljic, V. V. Shvartsman, D. C. Lupascu, J.-F. Li, J. Rödel, *Adv. Funct. Mater.* **2013**, *23*, 4079.
- [46] H. Yang, C. Zhou, X. Liu, Q. Zhou, G. Chen, W. Li, H. Wang, *J. Eur. Ceram. Soc.* **2013**, *33*, 1177.
- [47] D. Damjanovic, F. Brem, N. Setter, *Appl. Phys. Lett.* **2002**, *80*, 652.
- [48] D. P. Almond, B. Chapman, G. A. Saunders, *Supercon. Sci. Technol.* **1988**, *1*, 123.
- [49] S. T. Zhang, M. H. Lu, D. Wu, Y. F. Chen, N. B. Ming, *Appl. Phys. Lett.* **2005**, *87*, 262907.
- [50] S. M. Selbach, M.-A. Einarsrud, T. Grande, *Chem. Mater.* **2009**, *21*, 169.
- [51] T. Rojac, A. Bencan, B. Malic, G. Tutuncu, J. L. Jones, J. E. Daniels, D. Damjanovic, *J. Am. Ceram. Soc.* **2014**, *97*, 1993.